Published in final edited form as:

Clin Cancer Res. 2019 November 01; 25(21): 6475–6486. doi:10.1158/1078-0432.CCR-18-3549.

Leukotriene synthesis is critical for medulloblastoma progression

Fang Du[1,2], **Larra Yuelling**[2], **Eric H. Lee**[2], **Yuan Wang**[1], **Shengyou Liao**[1], **Yan Cheng**[1,2], **Li Zhang**[1], **Chaonan Zheng**[1], **Suraj Peri**[3], **Kathy Q. Cai**[2], **Jessica M. Y. Ng**[4], **Tom Curran**[4], **Peng Li**[5], **Zeng-jie Yang**[2]

[1]–Laboratory of Molecular Neuropathology, College of Pharmaceutical Sciences, Soochow University, Suzhou, China

[2]–Cancer biology program, Fox Chase Cancer Center, Temple University Health System, Philadelphia, PA, USA

[3]–Biostatistics and bioinformatics research facility, Fox Chase Cancer Center, Temple University Health System, Philadelphia, PA, USA

[4]–Children's Research Institute, Children's Mercy Kansas City, MO, USA

[5]–Department of Pharmacognosy and traditional Chinese pharmacology, College of Pharmacy, Army Medical University, Chongqing, China

Abstract

Purpose: Here, we examined the role of leukotriene, well-known inflammatory mediators, in the tumorigenesis of hedgehog pathway-associated medulloblastoma (MB), and tested the efficacies of antagonists of leukotriene biosynthesis in MB treatment.

Experimental Design: We examined the leukotriene levels in MB cells by ELISA. We next tested whether leukotriene synthesis in MB cells relied on activation of hedgehog pathway, or the presence of hedgehog ligand secreted by astrocytes. We then investigated whether leukotriene mediated hedgehog-induced Nestin expression in tumor cells. The functions of leukotriene in tumor cell proliferation and tumor growth in MB were determined through knocking down 5-lipoxygenase (a critical enzyme for leukotriene synthesis) by shRNAs, or using 5-lipoxygenase deficient mice. Finally, the efficacies of antagonists of leukotriene synthesis in MB treatment were tested *in vivo* and *in vitro*.

Results: Leukotriene was significantly up-regulated in MB cells. Increased leukotriene synthesis relied on hedgehog ligand secreted by astrocytes, a major component of MB microenvironment. Leukotriene stimulated tumor cells to express Nestin, a cytoskeletal protein essential for MB growth. Genetic blockage of leukotriene synthesis dramatically suppressed MB cell proliferation and tumor growth *in vivo*. Pharmaceutical inhibition of leukotriene synthesis markedly repressed MB cell proliferation, but had no effect on proliferation of normal neuronal progenitors. Moreover,

Corresponding author: Dr. Zeng-Jie Yang, Cancer Biology Program, Fox Chase Cancer Center, 333 Cottman avenue, Philadelphia, PA 19111, USA. Tel.: +1 215 214 1545; Fax: +1 215 728 2741; zengjie.yang@fccc.edu.

Disclosure of potential conflicts of interest

No potential conflicts were disclosed by the authors.

antagonists of leukotriene synthesis exhibited promising tumor inhibitory efficacies on drug-resistant MB.

Conclusions: Our findings reveal a novel signaling pathway that is critical for MB cell proliferation and tumor progression, and that leukotriene biosynthesis represents a promising therapeutic target for MB treatment.

Introduction

Medulloblastoma (MB) is a malignant tumor of developing cerebellum, representing a major cause of childhood morbidity and mortality [1]. Current treatment for MB consists of a combined modality approach including surgery, chemotherapy and radiation therapy. Despite aggressive treatment, a significant number of MB patients still succumb to this disease. Moreover, tumor treatment can cause delayed complications that have profound effects on quality of life in survivors [2–4]. Clinical studies and research efforts are now focused on attempts to decrease treatment toxicity while improving the cure rate in MB patients.

Leukotrienes (LTs), well-known inflammatory mediators, possess a wide range of biological activities including leukocyte chemotaxis, vascular leakage, endothelial cell migration and astrocyte proliferation[5]. The synthesis of LT from substrate arachidonic acid (AA) is initiated by 5-lipoxygenease (Alox5) in concert with 5-lipoxygenase-activated protein (FLAP)[6] (Fig. 1a). Recent studies reveal that LTs are implicated in many pathological conditions such as allergic diseases, cardiovascular diseases and many cancers[7]. However, it is still unknown whether LTs are involved in MB tumorigenesis.

Here, we show that LT biosynthesis is elevated in MB cells, and that enhanced LT biosynthesis in tumor cells relies on sonic hedgehog (Shh) ligand secreted by astrocytes, a major component of the MB microenvironment. LTs in MB cells are responsible for the induction of Nestin, an intermediate filament protein, which is required for MB progression [8]. Genetic or pharmaceutical blockage of LT synthesis prevented Nestin expression and resulted in inhibition of MB cell proliferation *in vitro* and *in vivo*. Moreover, inhibition of LT synthesis exhibited anti-tumor efficacy in drug-resistant MB cells, but did not affect proliferation of normal cerebellar granule neuron precursors (GNPs). Our data reveal a novel tumor-specific signaling pathway for LT-induced Nestin expression, which is essential for MB cell proliferation. Given the excellent safety profile, low cost, and ready availability of LT inhibitors, LT synthesis represents a promising therapeutic target for treatment of MB and perhaps other malignancies involving activation of the hedgehog (Hh) pathway.

Methods

Animals

Ptch1$^{fl/fl}$ mice have been described previously[9]. Alox5 null mice, *Ptch1*+/− mice, *Math1-Cre* mice, *P53* null mice and *R26R-SmoM2* mice were purchased from the Jackson Laboratory. *CB17/SCID* mice were bred in the Fox Chase Cancer Center Laboratory Animal Facility (LAF). All animals were maintained in the LAF at Fox Chase Cancer Center and all

experiments were performed in accordance with procedures approved by the Fox Chase Cancer Center Animal Care and Use Committee.

Chemicals, cell culture and proliferation assays

MB cells were isolated and cultured with NB-B27 medium in poly-D-lysine coated 96-well plate as described previously[9]. Smo antagonist, vismodegib was purchased from Cellagen technology. MK886, arachidonic acid, Cysteinyl LTs, LTA4-E4, montelukast and zileuton were obtained from Cayman Chemical. Cell proliferation assays were performed using Thiazolyl Blue Tetrazolium Bromide (MTT) (Sigma). Briefly, cells were seeded in flat bottom 96-well plates at a density of $4x10^5$ cells per well in 100 μl of NB-B27 medium in the presence of MK886 or vismodegib accordingly. After treatment for 48 hours, the culture medium was aspirated and replaced with 100μl per well of MTT (5mg/mL) diluted in NB-B27 medium at a 1:10 ratio. Reduction of MTT by living cells was determined after 4hrs of incubation by the difference in absorbance between 570nm and 655nm using an iMark microplate reader (BioRad).

Western blotting

Cells and tissues were lysed in RIPA buffer (Thermo) supplemented with protease (Roche) and phosphatase (Thermo) inhibitors cocktail. Total protein lysates were separated in 8% SDS-PAGE and transferred on PVDF membrane. Membranes were probed with antibodies against Alox5 (Cell Signaling, 1:1000), FLAP (cell signaling, 1:1000), GAPDH (Sigma-Aldrich, 1:1000). Western Blot signals were detected with SuperSignal West Pico Substrate and exposed on films.

qPCR

RNA was isolated using TRI reagent (Sigma-Aldrich) in RNase-free conditions. cDNA was synthesized using oligo(dT) and Superscript II reverse transcriptase (Invitrogen). Quantitative PCR reactions were performed in triplicates using iQ SYBR Green Supermix (Bio-Rad) and the Bio-Rad iQ5 Multicolor Real-Time PCR Detection System. Primer sequences are available upon request.

Immunofluorecent staining and Leukotriene enzyme immunoassay

Immunofluorescent staining of frozen sections and cells was carried out according to standard methods. Briefly, sections or cells were blocked and permeabilized for 2hrs with Phosphate buffered saline (PBS) containing 0.1% Triton X-100 and 1% normal goat serum, stained with primary antibodies overnight at 4°C, and incubated with secondary antibodies for 2 hrs at room temperature. Sections or cells were counterstained with DAPI and mounted with Fluoromount-G (Southern Biotech) before being visualized with a Nikon TE200 microscope.

Levels of endogenous leukotriene in GNPs and MB cells were measured using a leukotriene EIA kit (Cayman Chemical). Briefly, cells were lysed in 200μL of methanol, centrifuged to clear the lysate and then evaporated in a SpeedVac concentrator. After reconstitution in 100μl of EIA buffer, cysteinyl leukotriene content was assayed according to manufacturer's instructions.

Fluorescence activated cell sorting (FACs)

To purify astrocytes or macrophages/microglia, MB or postnatal cerebella were digested with 10U/ml papain (Worthington) and triturated to obtain a single cell suspension. Cells (at a density of 2-4x10^6/ml) were then stained on ice, for 1hr with primary antibodies and 30 mins with secondary antibodies, and analyzed by FACs.

An antibody against ACSA2 (astrocyte cell surface antigen 2, Cell Signaling, 1:200), was used to sort astrocytes. Antibodies against CD68 (Cell Signaling, 1:200) and CD11b (Abcam, 1:500) were used for macrophage/microglia purification.

Subcutaneous allografts

2x10^6 MB cells from *Math1-Cre/Ptch1$^{fl/fl}$* mice were mixed with matrigel, and subcutaneously injected into the hindflank of *CB17/SCID* mice. Tumor size was measured every two days, and tumor volume was calculated based on the formula: (W^2×L)/2 (W, width; L, length). Daily intraperitoneal injection of MK886 was started after the tumor volume reached 200mm^3. The animals were sacrificed when the tumor volume exceed 1cm^3. After sacrifice, tumors were collected and sectioned for immunohistochemistry analysis.

For experiments in figure 6f–6j, MK886 DMSO stock was dissolved in 0.5% methylcellulose 0.2% Tween-80. Drugs were administered by oral gavage using 24-G gavaging needles (Fine Science Tools, CA).

Statistical analysis

The raw gene expression data used for analyzing subtype specific pathway alterations in human MB (figure 1b and 1c) were obtained from GEO (GSE85218) and normalized using RMA. Gene set variation analysis (GSVA) on the RMA normalized expression data was applied to identify pathways that are enriched in a single sample (method arguments: function = gsva; mx. diff='TRUE'). 17799 gene sets compiled from all gene sets available in MsigDB, including KEGG and Biocarta pathways, were used for enrichment analysis. To identify pathways that differ significantly among subtypes, Kruskal–Wallis test was used to analyze the enrichment scores resulting from GSVA.

Student's *t* test was performed to determine the statistical significance of the difference in means between samples. Extra sum-of-squares F test was used to analyze the difference in cell proliferation between *SmoM2* MB cells and *ptch1*-deficient MB cells in figure 5j. $p<0.05$ was considered statistically significant. Error bars represent the SEM. Difference in tumor volume increase in figure 4a was assessed using the Kaplan-Meier survival analysis and the mantel-Cox log-rank test was used to assess the significance of difference between two cohorts of tumor bearing mice. Data handling and statistical processing was performed using Microsoft Excel and Graphpad Prism Software.

Results

1) LT synthesis was up-regulated in MB cells compared with GNPs.

Approximately 30% of human MB result from aberrant activation of the Shh pathway (Shh-MB) [10,11]. To investigate a possible association of LT synthesis with human Shh-MB, we performed Gene Ontology (GO) analysis using transcriptomes from 763 primary human MB including 223 Shh type (Shh-MB), 144 group 3, 326 group 4 and 70 Wnt tumors[12]. Among 17799 pathways analyzed (Supplementary Table S1), genes associated with LT biosynthesis and LT metabolism are markedly up-regulated in Shh group and Wnt group human MB cells compared with group 3 and group 4 ($p<0.001$) (Fig. 1b–1c). These data suggest that LT synthesis and metabolism may be involved in the tumorigenesis of Shh-MB and Wnt-MB. Shh-MB in this dataset consists of four distinct subgroups: 65 Shh-α, 35 Shh-β, 76 Shh-γ, 47 Shh-δ. As shown in figure 1d, tumor cells from the Shh β group express most elevated levels of Alox5, the critical enzyme for LT biosynthesis, indicating that LTs may be associated with clinical and/or cytogenetic features of this subgroup of Shh-MB [13].

Mice heterozygous for patched 1 (*ptch1*, an antagonizing receptor of hedgehog) are widely utilized as a model for Shh-MB, as 15-20% of these mice (*ptch1*+/− mice) develop MB in their cerebella by 3-4 months of age [14]. Targeted deletion of the *ptch1* gene in cerebellar GNPs causes MB formation with 100% penetrance[9,15,16], indicating that GNPs can serve as the cell of origin for Shh-type MB. We examined the level of LTs in MB cells freshly isolated from *ptch1*+/− mice by ELISA. GNPs from wild type cerebella at postnatal day 6 (P6) were used as a control. As shown in figure 1e, the amount of LTs was significantly increased in MB cells compared with GNPs, indicating that LT synthesis was elevated in MB cells. However, comparable levels of Alox5 and FLAP proteins were detected in GNPs and MB cells, suggesting that increased LT synthesis in MB cells was not due to up-regulation of Alox-5 and FLAP expression (Fig. 1f). It was previously reported that macrophage/mciroglia can produce LTs [7]. To exclude the possibility that observed up-regulation of LT biosynthesis in MB cells was due to contamination of macrophage/microglia, we examined the presence of macrophage/microglia in isolated MB cells and GNPs by FACs. As shown in supplementary figure S1a–S1b, comparable percentage of macrophage/microglia (CD68+ and CD11b+) was found in isolated MB cells and GNPs (0.26±0.04% in GNPs vs 0.26±0.08% in MB cells, $p>0.05$). Moreover, no difference in the LT biosynthesis of macrophage isolated from postnatal cerebella and tumor tissue was observed (Supplementary Fig. S1c). The above data suggest that elevated levels of LTs found in MB cells were not caused by macrophage/microglia present in isolated tumor cells.

2) Astrocyte-derived Shh stimulated LT synthesis in GNPs and MB cells

Having observed increased LT biosynthesis in MB cells compared with GNPs, we investigated whether enhanced synthesis of LT in MB cells was due to *ptch1* deficiency. For this purpose, we isolated cerebellar GNPs from mice carrying a Cre-deletable allele of *ptch1* (*ptch1*$^{fl/fl}$ mice)[17], and infected them *in vitro* with a lentivirus carrying a GFP-tagged Cre recombinase or an empty GFP construct as a control. As shown in figure 2a, the Shh pathway was activated in GNPs following infection with Cre recombinase, as evidenced by elevated expression of Shh pathway target genes such as *gli1* and *ptch2*. However,

comparable levels of LT were detected in *ptch1*-deficient GNPs and control cells (Fig. 2b), suggesting that *ptch1* deficiency alone is not capable of stimulating LT synthesis in GNPs. Astrocytes, a major cellular component in tumor microenvironment, promote MB cell proliferation and tumor growth by secretion of the Shh ligand [16]. To test whether astrocytes could induce LT synthesis in MB cells, we purified tumor-associated astrocytes from *ptch1*+/− mice by FACs using an antibody against astrocyte cell surface antigen 2 (ACSA2) [18], and harvested conditioned culture medium as previously described[16]. Then, *ptch1*-deficient GNPs were treated with astrocyte-conditioned culture medium (ACM) in the presence and absence of 5E1, an antibody that neutralizes the Shh ligand [19]. As shown in figure 2b, ACM markedly elevated LT synthesis in *ptch1*-deficient GNPs, and this effect was abrogated in the presence of 5E1. These data suggest that astrocytes stimulate LT biosynthesis in *ptch1*-deficient GNPs through Shh secretion.

To further examine whether Shh ligand can promote LT synthesis in MB cells, MB cells from *ptch1*+/− mice and GNPs from wild type cerebella at P6, were treated *in vitro* with 3ug/mL recombinant Shh for the designated time periods. The level of LT synthesis markedly increased in MB cells at 10 mins or 2hrs following treatment with recombinant Shh (Fig. 2c). The short time-frame associated with increased LT biosynthesis upon Shh treatment suggests that *de novo* transcription is not required. As shown in figure 2d, comparable levels of Alox5 protein were observed in MB cells either treated with Shh or with vehicle control. Shh-induced LT synthesis was also observed in GNPs (Fig. 2e), although the overall level of LT in GNPs was much lower than that in MB cells, implying that *ptch1* deletion is not necessary for Shh-stimulated LT synthesis in tumor cells. Our finding that Shh-induced LTs biosynthesis in MB cells does not require increased Alox5 expression, is consistent with a previous report indicating that Shh stimulated LT synthesis in mouse fibroblasts is independent of transcription [20,21].

3) LT mediated Shh-induced Nestin expression in MB cells

Our recent studies demonstrate that astrocyte-derived Shh promotes MB growth by stimulating tumor cells to express Nestin, a type VI intermediate filament protein [16]. Having observed that Shh can induce LT synthesis in MB cells, we sought to investigate whether LTs mediate Nestin induction in MB cells. We previously reported that approximately 20% of GNPs started expressing Nestin in *ptch1* deficient mice at P6, by utilizing conditional *ptch1*-mutant mice expressing CFP in Nestin positive cells (*Math1-Cre/ptch1$^{fl/fl}$/Nestin-CFP* mice) [8]. We fractionated Nestin positive (CFP+) and negative GNPs (CFP-) from *Math1-Cre/ptch1$^{fl/fl}$/Nestin-CFP* mice at P6 by FACs as previously described [8]. The level of LTs in Nestin positive *ptch1*-deficient GNPs were significantly elevated compared to those in Nestin negative counterparts, suggesting that *ptch1*-deficient GNPs increased LT synthesis as they expressed Nestin (Fig. 3a). Nestin negative GNPs were treated with exogenous Shh alone, together with MK886, a selective antagonist of FLAP [22], or with nordihydroguaiaretic (NDGA), a lipoxygenase inhibitor [23]. After treatment for 48hrs, GNPs were harvested to examine Nestin expression by immunocytochemistry. Consistent with our previous report[16], dramatic expression of Nestin protein was observed in those *ptch1*-deficient GNPs after Shh treatment (Fig. 3b–3c). However, MK886 or NDGA significantly repressed Shh-induced Nestin expression in GNPs (Fig. 3d–3f), suggesting that LT synthesis is required for Shh-

stimulated Nestin expression in *ptch1*-deficient GNPs. To test whether Shh-induced Nestin expression observed in GNP culture came from astrocytes, we isolated Nestin negative GNPs from *Math1-Cre/ptch1*$^{fl/fl}$*/Nestin-CFP* mice at P6, and treated them with Shh *in vitro* for 48hrs. GNP culture was then harvested to examine Nestin expression as well as the presence of astrocytes by immunocytochemistry. As shown in supplementary figure S2a–S2c, a few astrocytes expressing brain lipid-binding protein (BLBP), glial fibrillary acidic protein (GFAP) or S100 were detected in the culture, which did express Nestin protein. However, these cells account for less than 1% cells in the culture. These data exclude the possibility that Nestin induction in GNP culture after Shh treatment was due to the presence of astrocytes.

Cerebellar GNPs from *ptch1*$^{fl/fl}$ mice or wild type mice at P6, were infected with a lentivirus carrying a GFP-tagged Cre recombinase or an empty GFP construct as a control. Following the infection, GNPs were treated with LT or vehicle control (DMSO) for 48hrs. Extensive expression of Nestin protein was found in *ptch1*-deficient GNPs after LT treatment (Fig. 3g–3h), further confirming that LT is capable of inducing Nestin expression in GNPs after *ptch1* deletion. However, LT failed to stimulate Nestin expression in wild type GNPs (Fig. 3i), suggesting that LT-induced Nestin expression in GNPs relies on Shh pathway activation. Nestin mRNA and protein expressions in *ptch1*-deficient GNPs after LT treatment, were further confirmed by q-PCR and western blotting (Fig. 3j). The above GNPs were also harvested to examine Shh pathway activation by q-PCR. As shown in figure 3k, expression levels of *gli1* mRNA were much higher in *ptch1*-defient GNPs compared with wild type GNPs at 48hrs following the infection, suggesting that Shh pathway was activated in GNPs after deletion of *ptch1*. Although comparable levels of *gli1* mRNA expression was observed in *ptch1*-deficient GNPs after treatment with LTs or vehicle for 48hrs, LT treatment markedly increased *gli1* expression in *ptch1*-deficient GNPs compared with vehicle treatment at 72hrs. These data suggest that LT treatment sustains Shh signaling in *ptch1*-deficient GNPs, consistent with the functions of Nestin protein in maintaining Shh pathway activation[8].

Having observed that LT induced Nestin expression in GNPs only after *ptch1* deletion, we next tested whether Smo activation is required for LT-stimulated Nestin expression. *ptch1*-deficient GNPs were treated with LT together with vismodegib, a specific Smo antagonist[24], or DMSO control. 48hrs later, cerebellar GNPs were harvested to detect Nestin expression by immunocytochemistry. As shown in figure 3l, vismodegib repressed LT-induced Nestin expressions in *ptch1*-deficient GNPs. These data suggest that Smo activation is necessary for LT-induced Nestin expression, consistent with our recent finding that Smo activation was required for Shh-induced Nestin expression in MB cells [16]. Collectively, the above data demonstrate that LT synthesis is required for Shh-induced Nestin expression in MB cells.

4) LT synthesis is required for MB cell proliferation and tumor growth

We previously demonstrated that Nestin expression is critical to sustain MB cell proliferation as well as tumor growth [8,25,26]. In light of the important role of LT in Nestin induction in MB cells, we then examined the possible function of LT in MB cell proliferation. MB cells from *ptch1*+/− mice were infected with a lentivirus carrying Alox5

shRNAs or scrambled shRNAs. The efficiency of Alox5 knockdown in MB cells by shRNAs was confirmed by western blotting (Fig. 4a). 48hrs following virus infection, MB cells were harvested to examine the proliferation by immunocytochemistry with an antibody against Ki67 (Fig. 4b–4c). More than 80% of MB cells infected with scrambled shRNA were found positive for Ki67, compared with approximately 20% of tumor cells infected with Alox5 shRNAs (Fig. 4d). No obvious cell death or apoptosis was observed in MB cells after virus infection (supplementary Fig. S3a–S3b). The dramatic reduction in proliferation of MB cells after Alox5 knockdown (Fig. 4d), indicates that proliferation of MB cells depends on LT synthesis.

We next examined whether LT deficiency alters MB growth *in vivo*. For this purpose, we crossed *Math1-Cre/ptch1*$^{fl/fl}$ mice with Alox5 deficient mice (*Alox5 null*), which carry a germline mutation in the Alox5 gene [27]. No obvious alterations in the proliferation of GNPs and cerebellar structure were observed in Alox5 null mice compared with their wild type counterparts at P6, implying that LTs are not required for normal GNP proliferation (supplementary Fig. S4) [27]. Consistent with our previous reports [15,28], *ptch1* deletion significantly prolonged the proliferation of cerebellar GNPs, resulting in an enlarged cerebellum in *Math1-Cre/ptch1*$^{fl/fl}$ mice (Fig. 4e). At 8 weeks of age, tumor cells in *Math1-Cre/ptch1*$^{fl/fl}$ cerebella were actively proliferating (Ki67+, figure 4f), and they extensively expressed Nestin (Fig. 4g–4h). However, Alox5 deletion dramatically reduced GNP proliferation in *Math1-Cre/ptch1*$^{fl/fl}$*/Alox5 null* cerebella, leading to only a few ectopic lesions present in mutant cerebella (Fig. 4i–4j). Both proliferation and Nestin expression in GNPs were markedly inhibited (Fig. 4k–4l). Finally, tumor latency was significantly prolonged in *Math1-Cre/ptch1*$^{fl/fl}$*/Alox5 null* mice (median survival, 126 days) compared with that in *Math1-Cre/ptch1*$^{fl/fl}$ mice (median survival, 58 days, $p<0.0001$) (Fig. 4m). These data indicate that deficiency in LT synthesis inhibited MB growth by compromising tumor cell proliferation.

A small proportion of ectopic cells in Alox5 null cerebellum was still proliferative (Fig. 4k), which continued their proliferation and finally result in tumors with 100% penetrance (supplementary Fig. S5a). Tumor cells developed from Alox5-null, *ptch1*-mutant mice, still expressed Nestin and were highly proliferative (supplementary Fig. S5b–S5d). Moreover, expression of *gli1* and *ptch2* mRNAs was significantly up-regulated in tumor cells compared with GNPs (supplementary Fig. S5e), suggesting that Shh pathway was still activated in MB cells in Alox5-null *ptch1*-mutant mice.

5) Antagonist of LT synthesis inhibited MB cell proliferation

We next examined whether antagonism of LT synthesis can be utilized to treat MB. MB cells isolated from *ptch1*+/− mice, were treated with DMSO, MK886 or together with LT or arachidonic acid (AA) for 48hrs. As shown in figure 5a, more than 80% of MB cells were found proliferative (Ki67+) in control group (DMSO treated). Majority of tumor cells highly expressed Nestin, as expected. MK886 significantly repressed Nestin expression in tumor cells and inhibited MB cell proliferation (Fig. 5b), consistent with the critical role of Nestin in tumor cell proliferation [8]. Exogenous LT effectively rescued Nestin expression as well as proliferation of tumor cells repressed by MK886 (Fig. 5c). Because synthesis of LT from

AA still relies on Alox5 activity, AA failed to restore MK886-repressed Nestin expression or proliferation of MB cells (Fig. 5d–5e). Reduced expression of Nestin and compromised proliferation in MB cells was also observed following treatment with zileuton (supplementary Fig. S6a–S6e), a specific antagonist of Alox5 [29]. The above data suggest that endogenous leukotriene synthesis is necessary for Nestin expression and proliferation of MB cells.

Since inhibition of LT synthesis prevents MB cell proliferation by blocking Nestin expression, we hypothesized that MK886 should not affect proliferation of wild type GNPs, which do not express Nestin [9,30,31]. To test this idea, GNPs from wild type cerebella were treated with recombinant Shh protein *in vitro* to maintain proliferation (Fig. 5f) [32]. As shown in figure 5g, vismodegib inhibited proliferation of both MB cells and wild type GNPs as previously reported [33,34]. Although MK886 treatment dramatically inhibited MB cell proliferation, the proliferation of wild type GNPs was not affected (Fig. 5h–5i). These results are consistent with lacks of phenotypes in GNPs proliferation in Alox5 null cerebella. The above data indicate that LT is required for the proliferation of MB cells but not GNPs, and that inhibition of LT synthesis prevents proliferation in a tumor cell-specific manner.

Most of the known small molecule inhibitors of the Shh pathway (SANT1, CUR61414, vismodegib, sonidegib, saridegib etc.) target Smo [34,35]. These inhibitors have displayed promising anti-tumor responses in MB and basal cell carcinoma, in which the Shh pathway is activated by mutation [36,37]. However, the emergence of resistant Smo mutations, which can result in tumor relapse after an initial response, has emerged as a clinical concern [38]. It has been reported that MB cells overexpressing activated form of Smo (SmoM2) represent tumor cells that are resistant to Smo antagonists [18,22]. As expected, vismodegib was active against MB cells derived from *ptch1*-deficient mice with an IC50 of 63nM, whereas it failed to inhibit SmoM2 MB cells (Fig. 5j). However, MK886 exhibited comparable anti-proliferative activity in *ptch1*-deficient MB cells as well as SmoM2 MB cells (figure 5j, IC50=1.8uM in *ptch1*-deficient MB cells and 2.0uM in SmoM2 MB cells). In addition, inhibition of tumor cell proliferation by MK886 was also observed in MB cells from *ptch1+/−/p53 null* mice (supplementary Fig. S7, IC50=1.7uM). These data suggest that inhibition of LT synthesis could be utilized to treat tumors with drug-resistant Smo mutations.

6) MK886 inhibited MB growth *in vivo*

Finally, we examined whether MK886 could prohibit tumor growth *in vivo*. For this purpose, we utilized a subcutaneous allograft MB model by transplanting MB cells into flanks of *CB17/SCID* mice [39]. After tumors were established (200-400mm^3), *CB17/SCID* mice were treated with intraperitoneal inoculation of MK886 or DMSO. As shown in figure 6a, no obvious inhibition of tumor growth was observed after treatment with 10mg/kg MK886. However, 20mg/kg and 40mg/kg MK886 significantly inhibited tumor growth, with 46% (p<0.0001) and 72% (p<0.0001) growth inhibition, respectively, compared with DMSO-treated tumors. As predicted, Nestin expression and MB cell proliferation dramatically decreased in tumor tissue following MK886 treatment, compared with controls (Fig. 6b–6c). MK886 treatment also significantly promoted neuronal differentiation (NeuN

+) among transplanted MB cells (Fig. 6d–6e). These data demonstrated that MK886 treatment can inhibit MB growth *in vivo*.

To exclude the possible off-target effects of MK886 in inhibiting MB growth, we also generated subcutaneous MB models by using tumor cells from *Math1-Cre/ptch1$^{fl/fl}$/Alox5 null* mice (at 14 weeks of age) as well as from *Math1-Cre/ptch1$^{fl/fl}$* mice (at 8 weeks of age). Once tumors were established, mice were treated with 40mg/kg MK886 by oral gavage, once a day for 2 weeks. As shown in supplementary figure S8, the growth of *ptch1* mutant MB cells was significantly repressed by MK886 treatment. However, Alox5-null, *ptch1*-mutant tumor cells continued to progress despite MK886 treatment. These data suggest that MK886 inhibited MB growth by targeting Alox5.

Finally, we treated *Math1-Cre/ptch1$^{fl/fl}$* mice with MK886 or DMSO by oral gavage. Starting from 6 week of age, tumor bearing mice were treated with DMSO or 20mg/kg/day MK886 for 2 weeks. As shown in figure 6f, MK886 dramatically reduced tumor volume compared with DMSO control. We examined Nestin expression in mutant cerebella by qPCR. As shown in figure 6g, much less Nestin mRNA expression was observed in the cerebella after MK886 treatment than after DMSO treatment, suggesting that MK886 repressed Nestin expression in tumor cells. The survival of ptch1 mutant mice was significantly prolonged after MK886 treatment compared with the control (Fig. 6h). Histological analysis revealed that massive proliferating tumor cells accumulated on cerebellar surface of *Math1-Cre/ptch1$^{fl/fl}$* after DMSO treatment; however, following MK886 treatment, the majority of tumor cells initiated differentiation (NeuN+) and migrated inward, resulting in fewer ectopic cells in the mutant cerebellum (Fig. 6i–6j). Most MB cells were actively proliferating (ki67+) with spontaneous differentiation (NeuN+) observed in tumor tissues after DMSO treatment (Fig. 6k). However, MK886 dramatically reduced tumor cell proliferation and promoted substantial differentiation in MB tissue (Fig. 6l). No significantly increased apoptosis was found in mutant cerebella after MK886 treatment (supplementary Fig. S9a–S9c). In addition, we treated *Math1-Cre/R26R-SmoM2* (SmoM2) mice with DMSO or 20mg/kg/day MK886 for 2 weeks. Tumor growth was significantly inhibited in SmoM2 mice following MK886 treatment (supplementary Fig. S10a). Proliferation of tumor cells was markedly repressed by MK886, compared with the DMSO control (supplementary Fig. S10b–S10f). These data further confirm the inhibitory effect of MK886 on MB growth.

Discussion

We previously reported that astrocytes promote MB growth through Shh secretion, and astrocyte-derived Shh induced Nestin expression in tumor cells[16]. Here, we demonstrate that LT, well-known inflammatory molecules, mediate Shh-induced Nestin expression in MB cells. Collectively, these findings reveal a novel pathway in tumor cells, which is essential for MB tumorigenesis. As summarized in figure 7, astrocyte-derived Shh stimulates LT biosynthesis in MB cells, which induces Nestin expression in tumor cells upon Smo activation. Nestin protein promotes MB cell proliferation by sustaining Hh pathway activation, as we previously demonstrated [8]. These findings establish a novel function of LT

in MB tumorigenesis, and highlight the important role of tumor microenvironment in MB progression.

In our studies, increased LT biosynthesis in tumor cells was observed within 10mins after Shh treatment. Moreover, no alterations in mRNA expression of Alox5 and FLAP were observed in MB cells in the presence of Shh. These data indicate that Shh induces LT synthesis in a transcription-independent manner. The capacity of Shh to induce LT synthesis independently of transcription was also observed during cytoskeletal rearrangement and migration of fibroblasts and NIH3T3 cells[20,21]. Shh rapidly enhanced LT synthesis in *ptch1*-deficient MB cells, implying that receptors other than ptch1 may react to extracellular Shh. Recent studies have shown that ptch2, a ptch1 paralog, can interact with Shh and regulate Shh signaling and functions such as chemotaxis[40] and tissue patterning[41]. Moreover, ptch2 was found to exert tumor suppressive functions in MB and basal cell carcinoma[42,43]. Further studies are warranted to investigate whether ptch2 is involved in Shh-induced LT biosynthesis in MB cells. Consistent with our findings, a recent study demonstrated that Smo activation stimulates PLA2 to trigger the release of AA, a precursor of leukotriene, in mouse fibroblasts within 2hrs [44], providing a possible mechanism for Shh-induced LT synthesis in MB cells.

Our studies demonstrated that LT promoted the proliferation of MB cells through stimulating Nestin expression. However, it is noteworthy that all Alox5-null *ptch1*-mutant mice finally developed MB, despite markedly prolonged tumor latency. MB cells still expressed Nestin protein and Shh pathway was activated in tumor cells, suggesting that MB cells in Alox5-null cerebella may have developed a LT-independent mechanism to support tumor cell proliferation. It is also possible that a rare population of MB cells has the intrinsic capacity to proliferate (and express Nestin) in the absence of LT.

LT stimulated extensive expression of Nestin mRNA and protein in *ptch1*-deficient GNPs. Moreover, MK886 or zileuton dramatically repressed Nestin expression in MB cells *in vitro* and *in vivo*. These data demonstrate that LT induce Nestin expression in tumor cells. No significant difference in the capacity of inducing Nestin expression in *ptch1*-deficient GNPs was found among LTB4, C4, D4 and E4, which appears to be more potent than LT4 in stimulating Nestin expression (supplementary Fig. S11). Vismodelgib effectively inhibited LT-induced Nestin expression in ptch1-deficient GNPs, indicating that Hh pathway activation is required for Nestin expression in GNPs upon LT treatment. However, combination of Shh and LT failed to induce Nestin expression in wild type GNPs (supplementary Fig. S12). These data imply that *ptch1* deficiency may be also indispensable for LT-induced Nestin expression.

It is generally believed that LT functions through interactions with two putative receptors, cysteinyl leukotriene type 1 (Cys-LT1R) and type 2 receptors (Cys-LT2R)[45]. No Cys-LT2R mRNA expression was detected in GNPs, MB cells, macrophage or astrocytes in MB tissue. Elevated expression of Cys-LTR1 mRNA expression was found in macrophages, compared with low levels of expression in GNPs, tumor cells and astrocytes (supplementary Fig. S13a). Montelukast, an antagonist of Cys-LT1R[46], effectively represses LT signaling in the airway, providing a routine treatment for asthma and bronchoconstriction[47]. However,

Nestin expression and proliferation in MB cells were not altered by montelukast treatment in our studies (supplementary Fig. S13b–S13c). In addition, LT-induced Nestin expression in *ptch1*-deficient cells was not affected after knocking down Cys-LT1R and Cys-LT2R by shRNAs (data not shown). These data suggest that Cys-LT1R or Cys-LT2R may not participate LT-induced Nestin expression in MB cells. No expression of leukotriene B4 receptor 1 (*Ltb4r1*) and receptor 2 (*Ltb4r2*) was observed in MB cells by q-PCR (supplementary Fig. 14). Previous studies have reported that leukotriene may function through the peroxisome proliferator activated receptors (PPARs), nuclear hormone receptors that act as ligand-activated transcription factors [48,49]. Among three PPAR subtypes (PPARα, PPARβ and PPARγ), PPARγ was demonstrated to induce the transcription of Nestin in neural stem cells, and to regulate their proliferation and differentiation [50,51]. It was previously reported that Shh signaling activation up-regulates the expression of PPARγ in cerebellar GNPs, suggesting that PPARγ is a target gene of Shh signaling in these cells [52]. The above evidence suggests that PPARγ may mediate leukotriene-triggered Nestin expression in *Ptc*-deficient GNPs. Future studies are warranted to further investigate the involvement of PPARs in leukotriene functions in MB cells.

Our studies reveal for the first time a critical role for LT in MB progression. It is intriguing that inhibition of LT synthesis by MK886 or zileuton prevented MB cell proliferation and *in vivo* tumor growth, but did not effect proliferation of wild-type GNPs. In our studies, normal proliferation of GNPs was not affected after genetic deletion of Alox5 gene in Alox5 null mice. These data indicate that LT biosynthesis may represent a promising target for treatment of MB. Importantly, with the recent FDA approval of vismodelgib for use in advanced basal cell carcinoma, and with multiple other Smo inhibitors in clinical trials, drug resistant Smo mutations are likely to become more prevalent. In the present study, inhibition of LT synthesis by MK886 prevented tumor cell proliferation independent of Smo. These data strongly support the clinical evaluation of LT antagonists in the treatment of *de novo* Shh pathway tumors and for patients who have acquired resistance to Smo inhibitors.

Supplementary Material

Refer to Web version on PubMed Central for supplementary material.

Acknowledge

We would like to thank A. Efimov, E. Nicolas, J. Pei and J. Oesterling for technical assistance. This research was supported NCI (CA178380 and CA185504 to Z. Yang), ACS RSG (RSG1605301NEC to Z. Yang), PA CURE Health Research Fund (CURE 4100068716 to Z. Yang), and National Natural Science Foundation of China (81572724 and 81573449 to L. Zhang, 81703538 and BK20170348 to Y. Wang, 81472596 to P. Li).

References

1. Ng JM & Curran T The Hedgehog’s tale: developing strategies for targeting cancer. Nature reviews. Cancer 11, 493–501 (2011). [PubMed: 21614026]
2. Pomeroy SL & Sturla LM Molecular biology of medulloblastoma therapy. Pediatr Neurosurg 39, 299–304 (2003). [PubMed: 14734863]
3. Taylor MD, et al. Molecular subgroups of medulloblastoma: the current consensus. Acta neuropathologica 123, 465–472. [PubMed: 22134537]

4. Ullrich NJ & Pomeroy SL Pediatric brain tumors. Neurol Clin 21, 897–913 (2003). [PubMed: 14743655]
5. Kanaoka Y & Boyce JA Cysteinyl leukotrienes and their receptors: cellular distribution and function in immune and inflammatory responses. J Immunol 173, 1503–1510 (2004). [PubMed: 15265876]
6. Borgeat P, Hamberg M & Samuelsson B Transformation of arachidonic acid and homo-gamma-linolenic acid by rabbit polymorphonuclear leukocytes. Monohydroxy acids from novel lipoxygenases. The Journal of biological chemistry 251, 7816–7820 (1976). [PubMed: 826538]
7. Peters-Golden M & Henderson WR Jr. Leukotrienes. The New England journal of medicine 357, 1841–1854 (2007). [PubMed: 17978293]
8. Li P, et al. Nestin Mediates Hedgehog Pathway Tumorigenesis. Cancer research 76, 5573–5583 (2016). [PubMed: 27496710]
9. Li P, et al. A population of Nestin-expressing progenitors in the cerebellum exhibits increased tumorigenicity. Nat Neurosci 16, 1737–1744 (2013). [PubMed: 24141309]
10. Northcott PA, Korshunov A, Pfister SM & Taylor MD The clinical implications of medulloblastoma subgroups. Nat Rev Neurol 8, 340–351 (2012). [PubMed: 22565209]
11. Gibson P, et al. Subtypes of medulloblastoma have distinct developmental origins. Nature 468, 1095–1099 (2010). [PubMed: 21150899]
12. Northcott PA, et al. Medulloblastoma comprises four distinct molecular variants. Journal of clinical oncology : official journal of the American Society of Clinical Oncology 29, 1408–1414 (2011). [PubMed: 20823417]
13. Cavalli FMG, et al. Intertumoral Heterogeneity within Medulloblastoma Subgroups. Cancer Cell 31, 737–754 e736 (2017). [PubMed: 28609654]
14. Goodrich LV, Milenkovic L, Higgins KM & Scott MP Altered neural cell fates and medulloblastoma in mouse patched mutants. Science 277, 1109–1113 (1997). [PubMed: 9262482]
15. Yang ZJ, et al. Medulloblastoma can be initiated by deletion of Patched in lineage-restricted progenitors or stem cells. Cancer Cell 14, 135–145 (2008). [PubMed: 18691548]
16. Liu Y, et al. Astrocytes Promote Medulloblastoma Progression through Hedgehog Secretion. Cancer research 77, 6692–6703 (2017). [PubMed: 28986380]
17. Ellis T, et al. Patched 1 conditional null allele in mice. Genesis 36, 158–161 (2003). [PubMed: 12872247]
18. Sharma K, et al. Cell type- and brain region-resolved mouse brain proteome. Nat Neurosci 18, 1819–1831 (2015). [PubMed: 26523646]
19. Sasai K, et al. Shh pathway activity is down-regulated in cultured medulloblastoma cells: implications for preclinical studies. Cancer research 66, 4215–4222 (2006). [PubMed: 16618744]
20. Bijlsma MF, Peppelenbosch MP, Spek CA & Roelink H Leukotriene synthesis is required for hedgehog-dependent neurite projection in neuralized embryoid bodies but not for motor neuron differentiation. Stem Cells 26, 1138–1145 (2008). [PubMed: 18292210]
21. Bijlsma MF, Borensztajn KS, Roelink H, Peppelenbosch MP & Spek CA Sonic hedgehog induces transcription-independent cytoskeletal rearrangement and migration regulated by arachidonate metabolites. Cell Signal 19, 2596–2604 (2007). [PubMed: 17884337]
22. Dixon RA, et al. Requirement of a 5-lipoxygenase-activating protein for leukotriene synthesis. Nature 343, 282–284 (1990). [PubMed: 2300173]
23. Pavani M, et al. Inhibition of tumoral cell respiration and growth by nordihydroguaiaretic acid. Biochemical pharmacology 48, 1935–1942 (1994). [PubMed: 7986205]
24. Frank-Kamenetsky M, et al. Small-molecule modulators of Hedgehog signaling: identification and characterization of Smoothened agonists and antagonists. J Biol 1, 10 (2002). [PubMed: 12437772]
25. Akiyama M, Matsuda Y, Ishiwata T, Naito Z & Kawana S Inhibition of the stem cell marker nestin reduces tumor growth and invasion of malignant melanoma. J Invest Dermatol 133, 1384–1387 (2013). [PubMed: 23389394]
26. Zhang Y, et al. Nuclear Nestin deficiency drives tumor senescence via lamin A/C-dependent nuclear deformation. Nat Commun 9, 3613 (2018). [PubMed: 30190500]

27. Chen XS, Sheller JR, Johnson EN & Funk CD Role of leukotrienes revealed by targeted disruption of the 5-lipoxygenase gene. Nature 372, 179–182 (1994). [PubMed: 7969451]
28. Gordon RE, et al. Statins Synergize with Hedgehog Pathway Inhibitors for Treatment of Medulloblastoma. Clinical cancer research : an official journal of the American Association for Cancer Research 24, 1375–1388 (2018). [PubMed: 29437795]
29. Carter GW, et al. 5-lipoxygenase inhibitory activity of zileuton. J Pharmacol Exp Ther 256, 929–937 (1991). [PubMed: 1848634]
30. Wojcinski A, et al. Cerebellar granule cell replenishment postinjury by adaptive reprogramming of Nestin(+) progenitors. Nat Neurosci 20, 1361–1370 (2017). [PubMed: 28805814]
31. Machold R & Fishell G Math1 is expressed in temporally discrete pools of cerebellar rhombic-lip neural progenitors. Neuron 48, 17–24 (2005). [PubMed: 16202705]
32. Wechsler-Reya RJ & Scott MP Control of neuronal precursor proliferation in the cerebellum by Sonic Hedgehog. Neuron 22, 103–114 (1999). [PubMed: 10027293]
33. Berman DM, et al. Medulloblastoma growth inhibition by hedgehog pathway blockade. Science 297, 1559–1561 (2002). [PubMed: 12202832]
34. Chen JK, Taipale J, Cooper MK & Beachy PA Inhibition of Hedgehog signaling by direct binding of cyclopamine to Smoothened. Genes & development 16, 2743–2748 (2002). [PubMed: 12414725]
35. Tao H, et al. Small molecule antagonists in distinct binding modes inhibit drug-resistant mutant of smoothened. Chemistry & biology 18, 432–437 (2011). [PubMed: 21513879]
36. Rudin CM, et al. Treatment of medulloblastoma with hedgehog pathway inhibitor GDC-0449. The New England journal of medicine 361, 1173–1178 (2009). [PubMed: 19726761]
37. Von Hoff DD, et al. Inhibition of the hedgehog pathway in advanced basal-cell carcinoma. The New England journal of medicine 361, 1164–1172 (2009). [PubMed: 19726763]
38. Yauch RL, et al. Smoothened mutation confers resistance to a Hedgehog pathway inhibitor in medulloblastoma. Science 326, 572–574 (2009). [PubMed: 19726788]
39. Kim J, et al. Itraconazole, a commonly used antifungal that inhibits Hedgehog pathway activity and cancer growth. Cancer Cell 17, 388–399 (2010). [PubMed: 20385363]
40. Alfaro AC, Roberts B, Kwong L, Bijlsma MF & Roelink H Ptch2 mediates the Shh response in Ptch1−/− cells. Development 141, 3331–3339 (2014). [PubMed: 25085974]
41. Zhulyn O, Nieuwenhuis E, Liu YC, Angers S & Hui CC Ptch2 shares overlapping functions with Ptch1 in Smo regulation and limb development. Developmental biology 397, 191–202 (2015). [PubMed: 25448692]
42. Lee Y, et al. Patched2 modulates tumorigenesis in patched1 heterozygous mice. Cancer research 66, 6964–6971 (2006). [PubMed: 16849540]
43. Veenstra VL, et al. Patched-2 functions to limit Patched-1 deficient skin cancer growth. Cell Oncol (Dordr) 41, 427–437 (2018). [PubMed: 29869097]
44. Arensdorf AM, et al. Sonic Hedgehog Activates Phospholipase A2 to Enhance Smoothened Ciliary Translocation. Cell reports 19, 2074–2087 (2017). [PubMed: 28591579]
45. Haeggstrom JZ & Funk CD Lipoxygenase and leukotriene pathways: biochemistry, biology, and roles in disease. Chem Rev 111, 5866–5898 (2011). [PubMed: 21936577]
46. Lynch KR, et al. Characterization of the human cysteinyl leukotriene CysLT1 receptor. Nature 399, 789–793 (1999). [PubMed: 10391245]
47. Leff JA, et al. Montelukast, a leukotriene-receptor antagonist, for the treatment of mild asthma and exercise-induced bronchoconstriction. The New England journal of medicine 339, 147–152 (1998). [PubMed: 9664090]
48. Narala VR, et al. Leukotriene B4 is a physiologically relevant endogenous peroxisome proliferator-activated receptor-alpha agonist. The Journal of biological chemistry 285, 22067–22074 (2010). [PubMed: 20400503]
49. Paruchuri S, et al. Leukotriene E4 activates peroxisome proliferator-activated receptor gamma and induces prostaglandin D2 generation by human mast cells. The Journal of biological chemistry 283, 16477–16487 (2008). [PubMed: 18411276]

50. Wada K, et al. Peroxisome proliferator-activated receptor gamma-mediated regulation of neural stem cell proliferation and differentiation. The Journal of biological chemistry 281, 12673–12681 (2006). [PubMed: 16524877]

51. Morales-Garcia JA, et al. Peroxisome proliferator-activated receptor gamma ligands regulate neural stem cell proliferation and differentiation in vitro and in vivo. Glia 59, 293–307 (2011). [PubMed: 21125653]

52. Bhatia B, et al. Hedgehog-mediated regulation of PPARgamma controls metabolic patterns in neural precursors and shh-driven medulloblastoma. Acta neuropathologica 123, 587–600 (2012). [PubMed: 22407012]

Translational Relevance

Medulloblastoma (MB), a pediatric brain tumor, often derives from aberrant activation of hedgehog pathway. Common strategies to inhibit hedgehog pathway are through targeting Smoothened (Smo) receptor. However, such approaches lack tumor selectivity and rapidly cause drug resistance due to Smo mutations. Therefore, two FDA-approved Smo antagonists, vismodegib and sonidegib, have not been therapeutically useful for MB treatment. Here we demonstrate leukotrienes, common inflammatory mediators, are essential for MB tumorigenesis. Antagonists of leukotriene biosynthesis dramatically inhibit tumor cell proliferation and repress tumor growth, but have no effects on the proliferation of normal neuronal progenitors or normal brain development. Moreover, leukotriene inhibitors exhibit intriguing efficacies on drug-resistant MB cells. Our findings demonstrate that leukotriene synthesis represents a novel therapeutic target for MB, and strongly support the clinical evaluation of leukotriene antagonists in the treatment of *de novo* hedgehog pathway tumors and for patients who have acquired drug resistance.

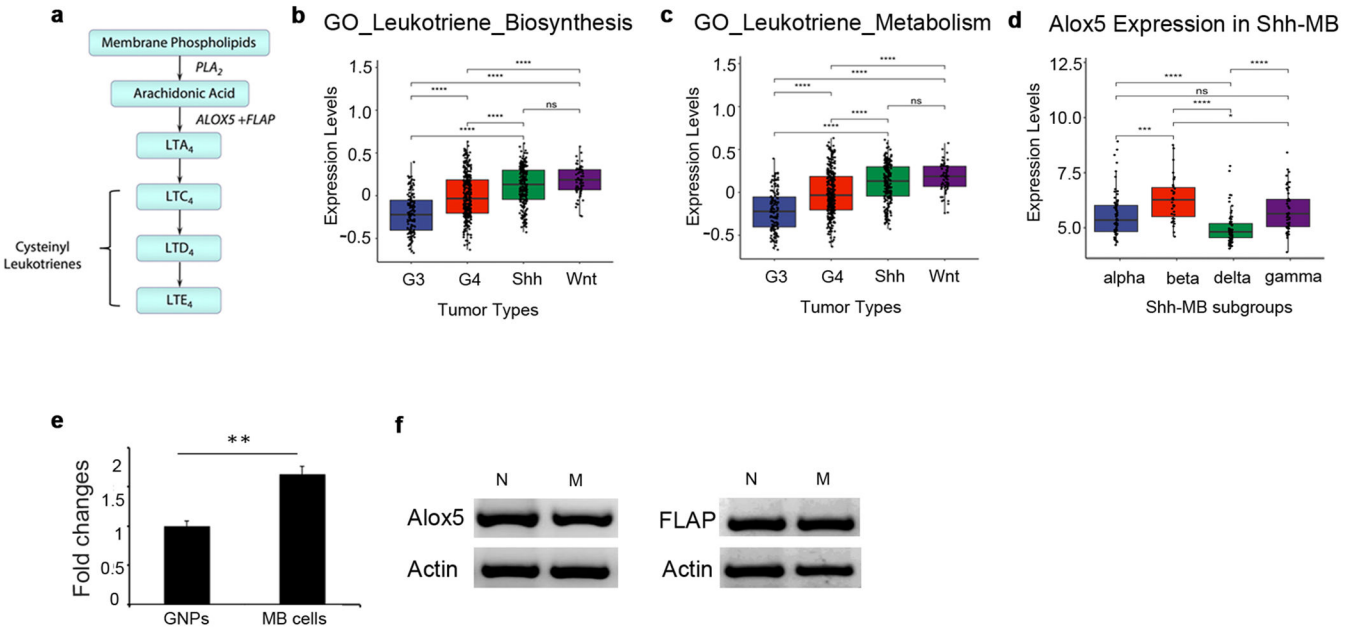

Figure 1. Increased LT synthesis in Shh-MB

a, Biosynthesis pathway of LTs. Arachidonic acid is derived from membrane phospholipid by phospholipase A2 (PLA2), and converted to leukotriene A4 (LTA4) by the action of Alox5 and FLAP. LTA4 is rapidly converted to cysteinyl LTs including LTC4, LTD4 and LTE4. b-c, Boxplots depicting the enrichment scores from gene set variation analysis (GSVA) for Gene Ontology groups: Leukotriene biosynthetic and metabolic processes (available from MsigDB (PMID: 24743996). x and y-axes illustrate enrichment score across 4 groups of human MB. Positive and negative scores indicate positive and negative enrichment, respectively. Pink dots represent the enrichment score for each sample in that subgroup. Black bar in the middle of the box indicates median. d, Alox5 expression levels in tumor cells from 4 subgroups of human Shh-MB. e, GNPs from wild type mice at P6 and MB cells from *ptch1*+/− mice were harvested to examine LT levels by ELISA. f. Expression of Alox5 and FLAP proteins in P6 GNPs (N) and MB cells (M) was examined by western blotting. ***, $p < 0.001$; ****, $p < 0.001$; ns, not significant.

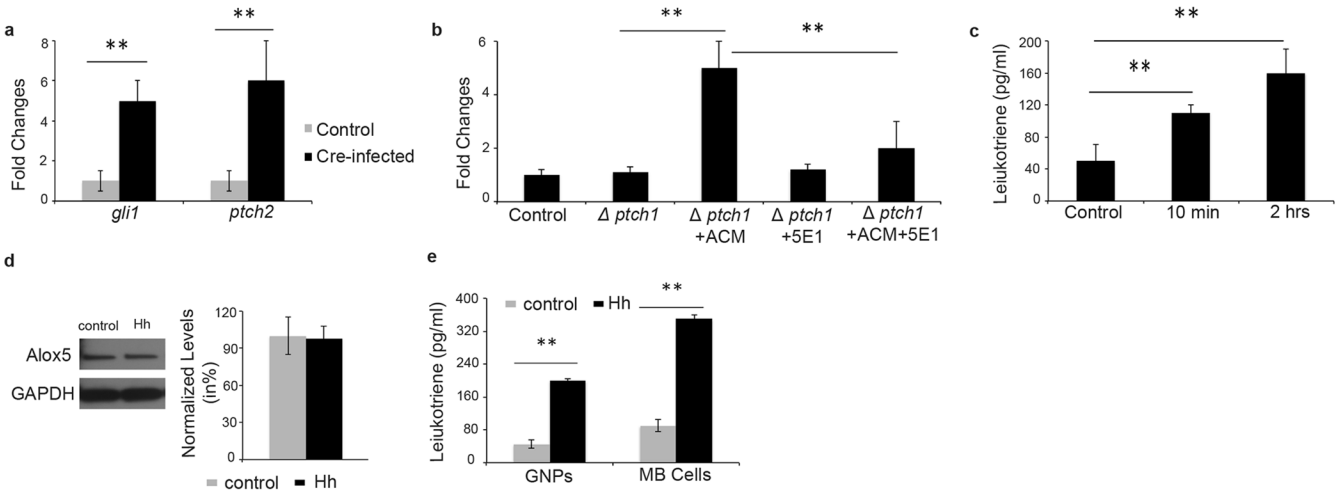

Figure 2. Shh stimulated LT synthesis in GNPs and MB cells

a. q-PCR analyses of *gli1* and *ptch2* expression in GNPs after infection with a lentivirus carrying Cre recombinase (Cre-infected) or an empty vector (control). b. Fold changes of LT amount in GNPs after *ptch1* deletion (Δ *ptch1*) and treated with ACM, or together with 5E1. c. Levels of LT in MB cells after Hh treatment *in vitro*, examined by ELISA. d. western blotting analyses of Alox5 protein expression in MB cells at 2hrs after treatment with Hh or control. e. LT Levels in GNPs and MB cells at 2hrs after treatment with Hh or control. **, $p<0.01$.

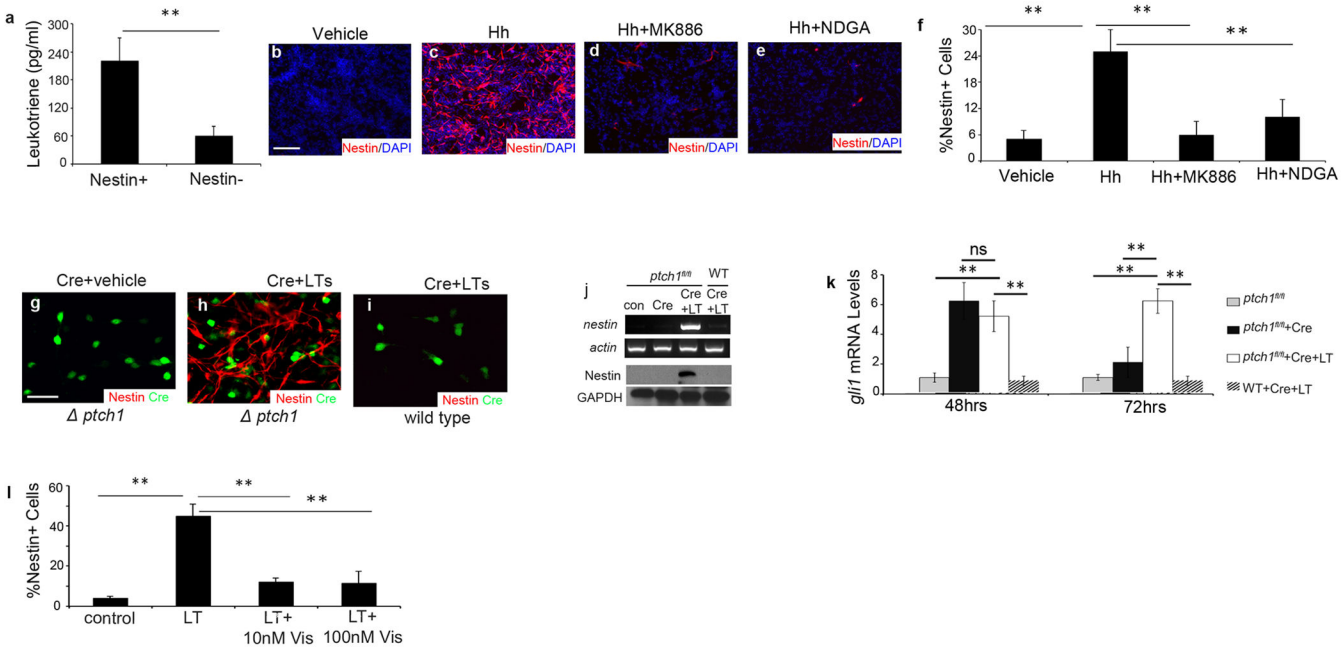

Figure 3. LT mediated Hh-induced Nestin expression in MB cells

a, LT levels in Nestin+ and Nestin− cell populations isolated from *Math1-Cre/ptch1*$^{fl/fl}$*/ Nestin-CFP* mice at P6. b-e, Nestin protein expression in *ptch1*-deficient GNPs after treatment with Hh, together with MK886 or NDGA by immunocytochemistry. DAPI was used to counterstain cell nuclei. f. Percentage of Nestin+ (CFP+) cells among *ptch1*-deficient GNPs after the treatment. g-i, Nestin expression in Cre-infected GNPs from P6 *ptch1*$^{fl/fl}$ mice (g-h) or wild type mice after treatment with 100nM LT. j, Nestin mRNA and protein expression in wild type or *ptch1*-deficient GNPs by qRT-PCR and western blotting. k, *gli1* mRNA expression in GNPs after designated treatment. l, percentage of Nestin+ cells among *ptch1*-deficient GNPs after treatment with LT or together with cyclopamine. **, $p<0.01$, scale bars, 50μm.

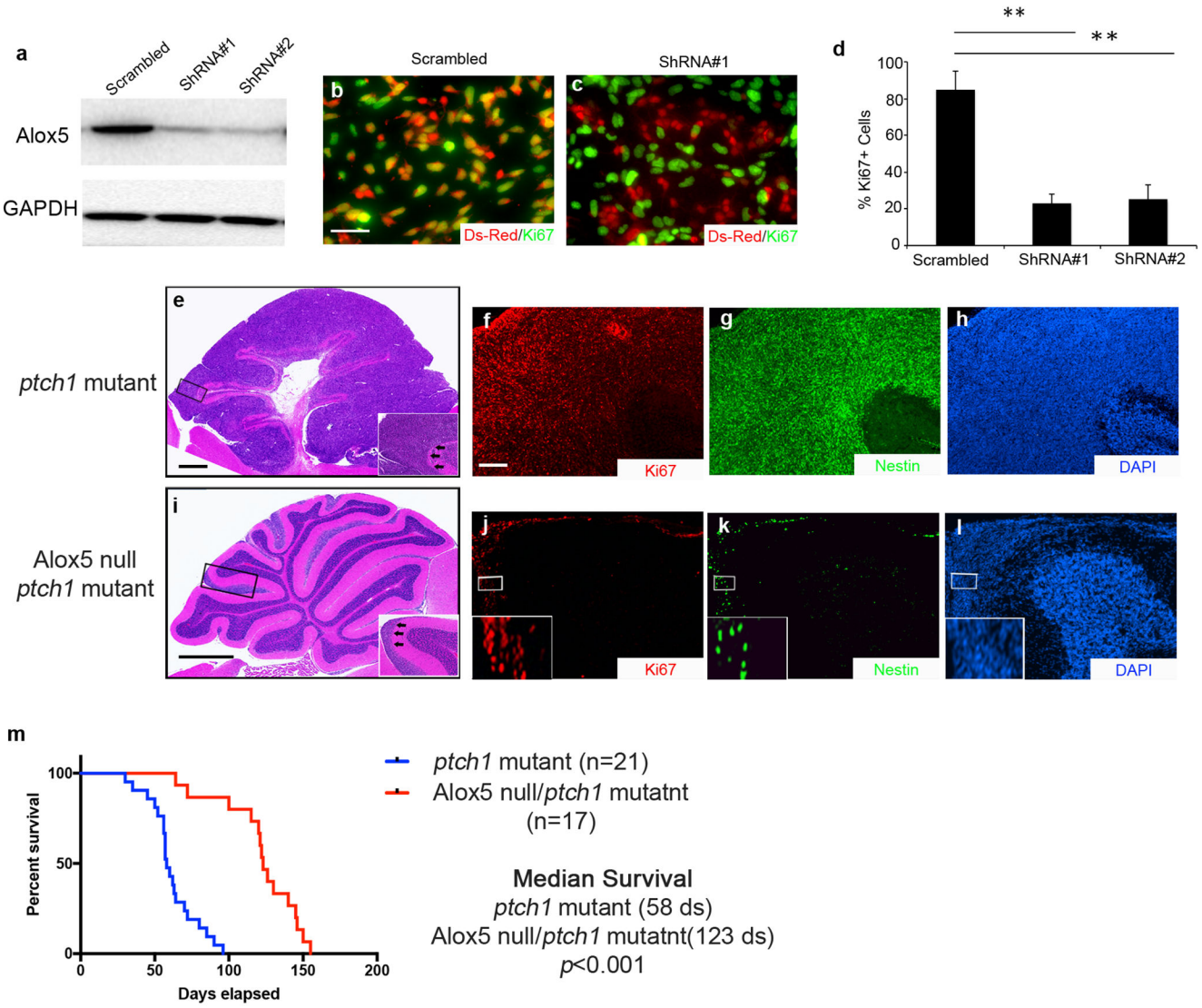

Figure 4. LT synthesis was required for MB growth

a. Expression of Alox5 and GAPDH proteins in MB cells infected with a lentivirus carrying scrambled shRNA or shRNAs specific for Alox5. b-c, immunocytochemistry analysis of Ds-Red and Ki67 protein in MB cells of control group (scrambled) or after Alox5 knockdown (shRNA#1). Ds-Red labels infected MB cells. d. Percentage of Ki67+ cells among MB cells infected with lentivirus carrying scrambled ShRNA or ShRNAs targeting Alox5. e-i, HE staining (e and i) and immunohistochemistry analysis of Ki67 (f and j) and Nestin (g and k) of sagittal sections of a *Math1-Cre/ptch1$^{fl/fl}$* cerebellum (e-h) and a *Math1-Cre/ptch1$^{fl/fl}$/Alox5 null* cerebellum (i-l) at 8 weeks of age. DAPI was used to counterstain cell nuclei (h and l). m. Kaplan-Meier survival curve of *Math1-Cre/ptch1$^{fl/fl}$* mice and *Math1-Cre/ptch1$^{fl/fl}$/Alox5 null* mice. Insets in e and i-l highlight tumor cells in boxes. Arrows in e and I point tumor cells. **, $p<0.01$. Scale bars in b and f, 50μm; in e and i, 200μm.

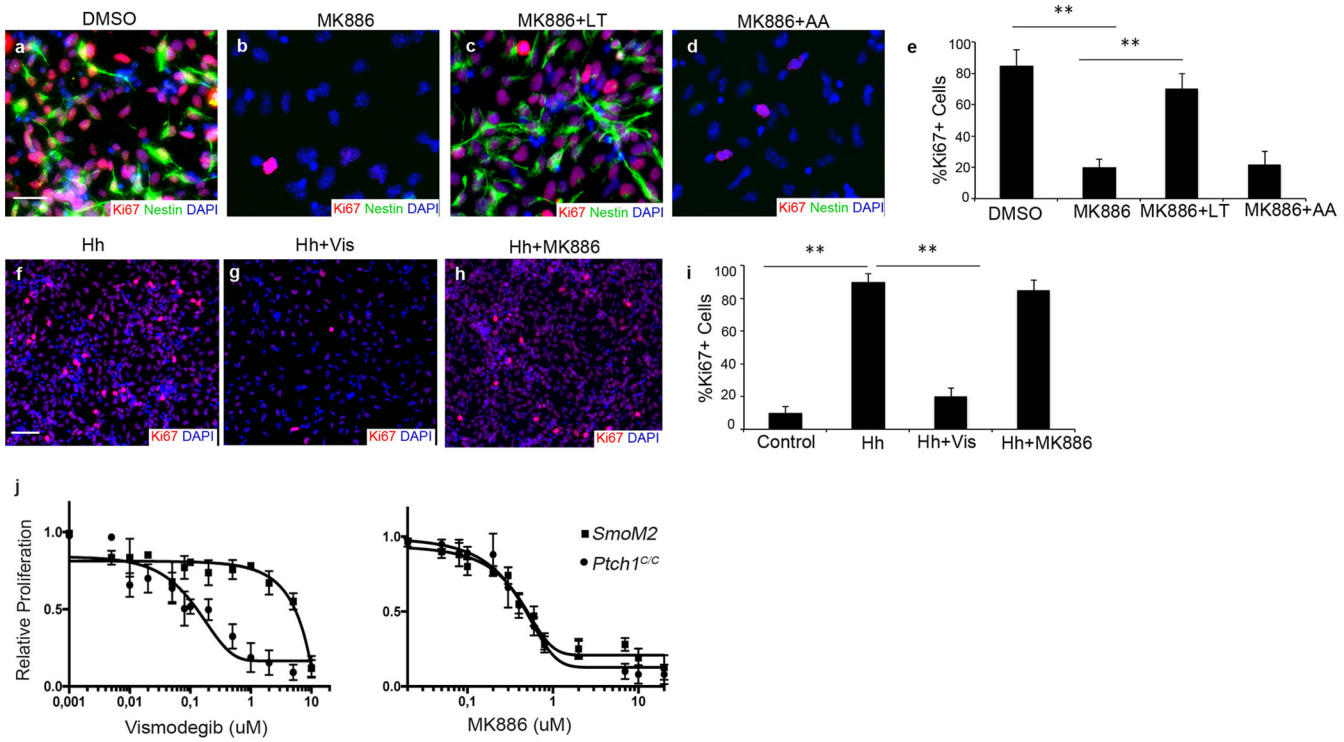

Figure 5. MK886 inhibited MB cell proliferation *in vitro*

a-e, MB cells were treated with DMSO (a), 2μM MK886 (b), 2μM MK886 and 80ng/ml LTs (c), and 2μM MK886 together with 2μM AA (d) for 48hrs, and immunostained for Ki67 and Nestin. DAPI was used to counterstain cell nuclei (a-d, f-h). Percentage of Ki67+ cells among cultured MB cells (a-d) was quantified in e. f-i, GNPs from P7 wild type mice were treated with 3μg/ml recombinant Shh alone (f), or together with 100nM vismodegib (g) or 300nM MK886 (h) for 48hrs, before immunostaining for Ki67. The percentage of Ki67+ cells was then quantified in i. j. Proliferation of MB cells isolated from *Math1-Cre/Ptch1*$^{fl/fl}$ mice (*Ptch1*-deficient MB) and *Math1-Cre/SmoM2* mice (SmoM2 MB) treated with increased dosages of vismodegib and MK886. **, $p<0.01$. Scale bars, 50μm.

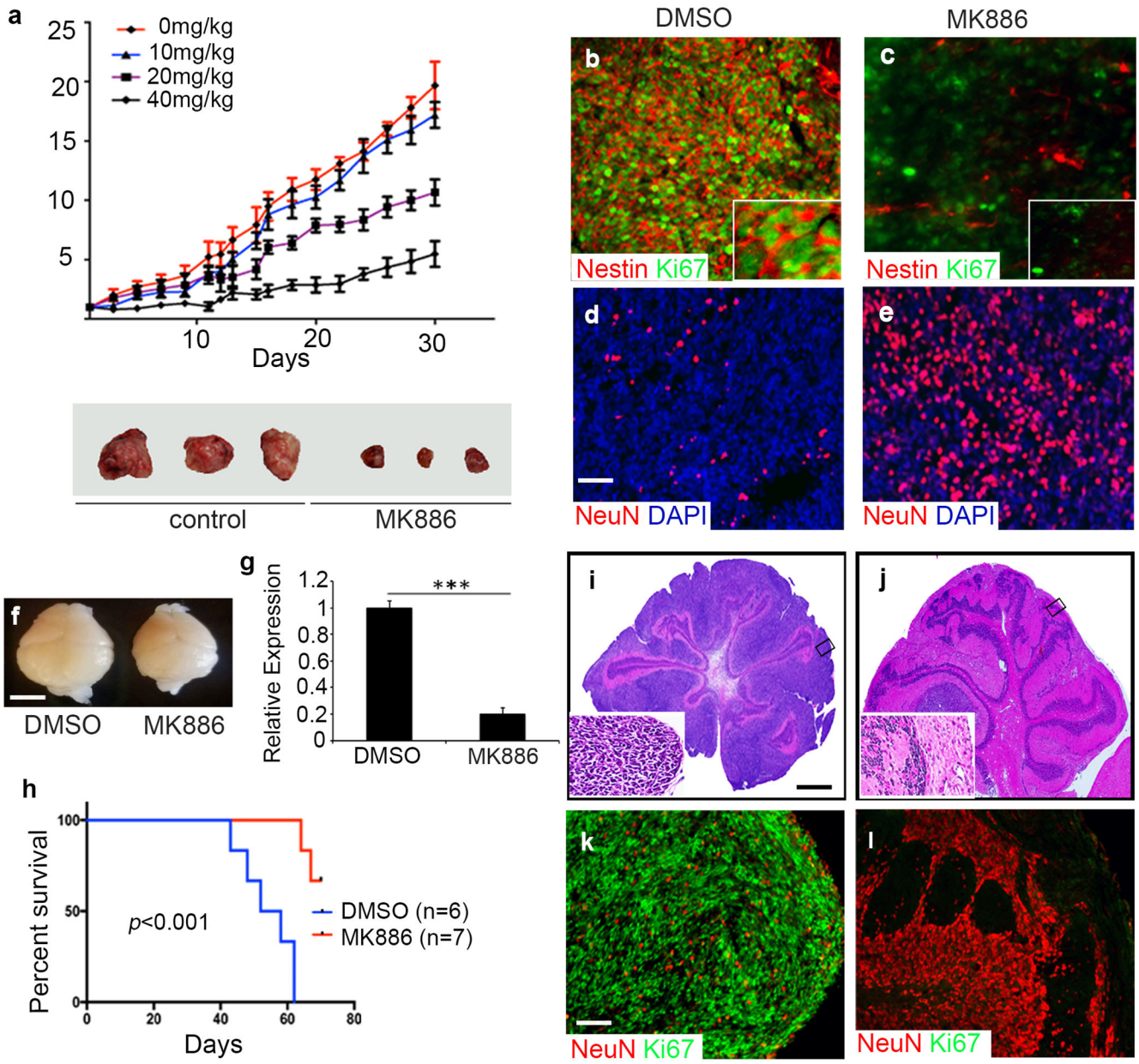

Figure 6. MK886 repressed tumor growth *in vivo*

a, *CB17/SCID* mice with established MB allografts were treated daily with DMSO or MK886 with designated dosages by intraperitoneal injection. Tumor volume was measured every two days and volume increase was quantified in fold. n=4 in each treatment group. Representative pictures of tumors from *CB17/SCID* mice after treatment with DMSO (control) and 40mg/kg MK886. b-e, MB tumors in *CB17/SCID* mice after completion of treatment with DMSO (b and d) or 40mg/kg MK886 (c and e), were sectioned to examine expression of Nestin and Ki67 (b-c), and NeuN by immunohistochemistry. DAPI was used to counterstain cell nuclei. Inserts in b and c, represent higher magnification of Nestin and Ki67 expression. f, whole mount images of cerebella from *Math1-Cre/Ptch1*$^{fl/fl}$ mice at 8 weeks of age, after oral treatment with DMSO (left) or MK886 (right) for 2 weeks. g,

relative levels of Nestin mRNA expression in MB tissue after treatment with DMSO or MK886, examined by qPCR. h, survival curve of *Math1-Cre/Ptch1$^{fl/fl}$* mice after the treatment with DMSO or MK886. i-l, HE staining of cerebellar sections of *Math1-Cre/Ptch1$^{fl/fl}$* mice treated with DMSO (i) or MK886 (j). Insets highlight cerebellar structure in boxes. k-l, Ki67 and NeuN expression in tumor tissue after treatment with DMSO (k) or MK886 (l), examined by immunohistochemistry. Scale bars, b-e and i-l, 50μm; f, 300μm. ***, $p<0.001$.

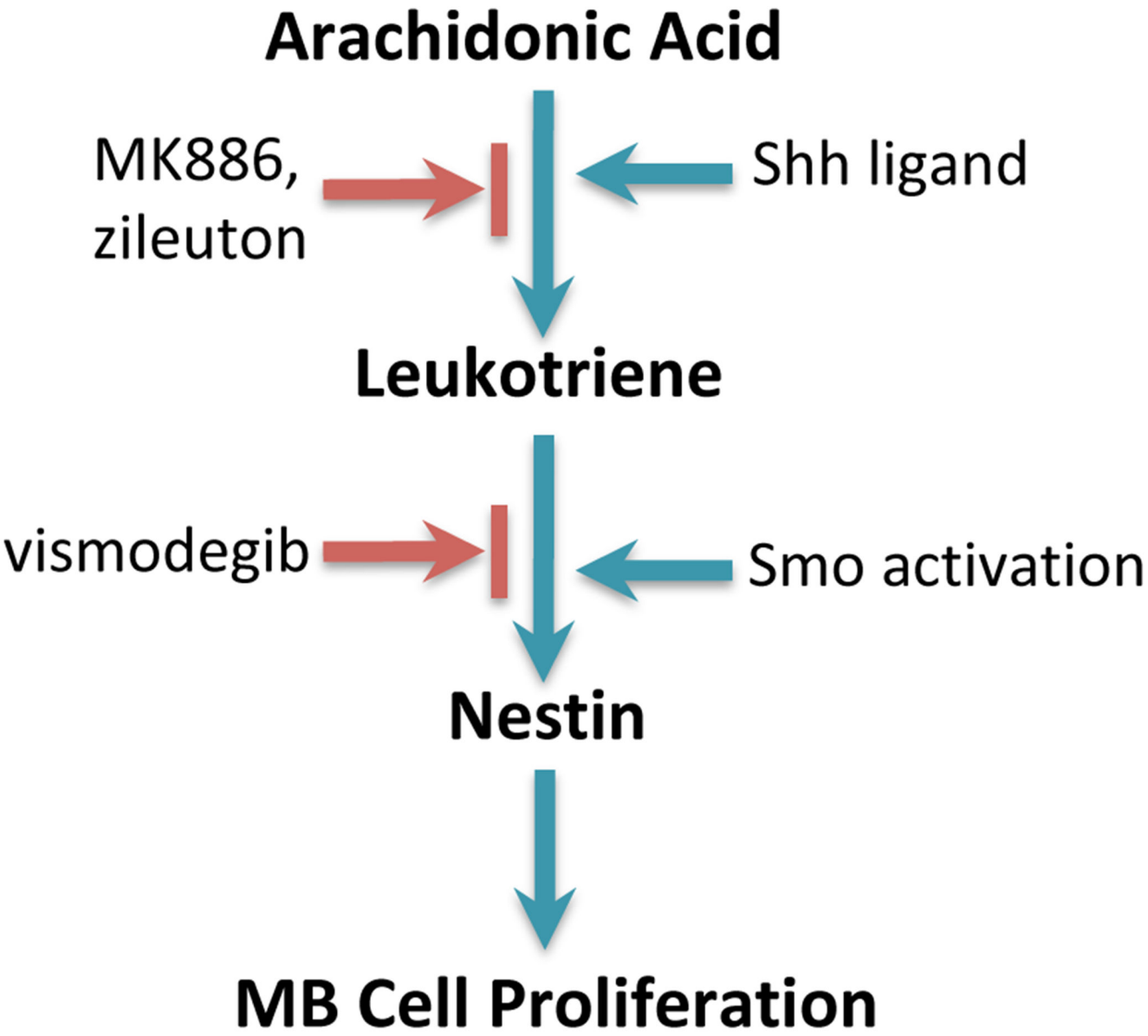

Figure 7. A schematic model for LT-induced Nestin expression in MB cells

Astrocyte-derived shh stimulates LT biosynthesis from arachidonic acid. Upon Smo activation, LT induces Nestin expression in tumor cells, thereby promotes tumor cell proliferation. LT synthesis in MB cells is blocked by MK886 or zileuton. Vismodegib inhibits LT-induced Nestin expression in MB cells.